lubricants

MDPI

Article

Lubricity Properties of Palm Oil Biodiesel Blends with Petroleum Diesel and Hydrogenated Vegetable Oil

Nur Allif Fathurrahman [1,2,*], Ahmad Syihan Auzani [3], Rizal Zaelani [1], Riesta Anggarani [2], Lies Aisyah [2], Maymuchar [2] and Cahyo Setyo Wibowo [2]

[1] NRE-Biofuel Laboratory, Department of Product Application Technology, Research and Development Center for Oil and Gas Technology (LEMIGAS), South Jakarta 12230, Indonesia
[2] Department of Product Application Technology, Research and Development Center for Oil and Gas Technology (LEMIGAS), South Jakarta 12230, Indonesia
[3] Department of Mechanical Engineering, Faculty of Engineering, University of Indonesia, Depok 16424, Indonesia; auzani@ui.ac.id
* Correspondence: nur.allif@ui.ac.id

Abstract: While the methyl ester structure in biodiesel is responsible for lubrication improvement in base fuels with poor lubricity properties such as ultra-low sulfur diesel and non-upgraded HVO, relatively little is known about its effect on all-level blends, which would provide higher energy security for biodiesel utilization. In this study, binary blends of palm oil biodiesel (POB) with commercial petroleum diesel fuel (DF) and HVO at every 10%-*v*/*v* blend point were analyzed using a high-frequency reciprocating rig (HFRR) according to the standard method of ASTM D6079. It was found that the addition of POB successfully improved the lubricating properties of DF-CN48 and DF-CN51 and efficiently acted as a lubricity improver that showed a minimum friction coefficient and improved the specific wear rate. The adsorption of ester molecules on the metallic surfaces acted as a protective layer during the rubbing process, resulting in lubricity improvement for the diesel fuel. Interestingly, the 60–90%-*v*/*v* POB blend with HVO showed a lubricity capacity that competed determinatively and attractively, resulting in a non-ideal contribution to the changes in the friction coefficient, WSD formation, and specific wear rate.

Keywords: biodiesel; diesel fuel blends; HVO; HFRR; lubricity

Citation: Fathurrahman, N.A.; Auzani, A.S.; Zaelani, R.; Anggarani, R.; Aisyah, L.; Maymuchar; Wibowo, C.S. Lubricity Properties of Palm Oil Biodiesel Blends with Petroleum Diesel and Hydrogenated Vegetable Oil. *Lubricants* **2023**, *11*, 176. https://doi.org/10.3390/lubricants11040176

Received: 6 March 2023
Revised: 30 March 2023
Accepted: 7 April 2023
Published: 12 April 2023

1. Introduction

1.1. Background

Diesel fuel is widely used for heavy-duty vehicles in the transportation and industry sectors. It provides higher thermodynamic efficiency and fuel economy compared with motor gasoline engines. In 2040, the global demand for diesel fuel is expected to increase to 1834 billion liters, according to data from the Organization of Petroleum Exporting Countries (OPEC) [1]. Unfortunately, burning diesel also contributes to global warming, ozone depletion, and air pollution. Therefore, diesel alternatives have been proposed to reduce the dependency on petroleum-based diesel and use more sustainable resources, such as vegetables and animal fats. However, using vegetable oil and animal fats directly causes engine problems due to their high viscosity [2,3]. Alternatively, transesterification and hydrotreatment processes can be applied to vegetable oils and animal fats to yield hydrotreated vegetable oil (HVO) and fatty acid methyl ester (FAME), which have more desirable properties for biodiesel. The trend of HVO production for the biodiesel supply increased from 5 percent in 2019 to 10 percent in 2021. Meanwhile, Indonesia's largest crude palm oil producer reported a continuous increase in production since 2015, with 48 million tons of CPO being produced in 2019. CPO resources potentially increase the size of the biodiesel supply. However, considering its sustainability, biodiesel production from CPO creates full life-cycle environmental issues. Therefore, using non-edible oils as

feedstocks for biodiesel production can reduce competition for food production resources and reduce greenhouse gas emissions. Moreover, the environmental impact of biodiesel synthesis from non-edible oils depends on factors such as the type of feedstock used, the energy source for production, and the disposal of waste products [4,5].

Many studies have reported that biodiesel has been proposed as a lubricity improver for a long time, opening a potential market [6]. It is fascinating if blended with other base fuels with poor lubricity properties, such as non-sulfur diesel and non-upgraded HVO [7,8]. The chemical composition of HVO consists of simple n-alkane. In contrast, diesel fuel consists of a complex mixture of hydrocarbons, resulting in a higher cetane number than HVO of approximately 69–75 [9], while the standard minimum is 40, based on ASTM D975. The heat release rate of HVO is higher than that of diesel fuel [9]. With the environmental benefits of HVO and palm oil biodiesel, these fuels are considered to be viable alternatives to diesel fuel. Furthermore, using biodiesel for lubricity improvement is an option for low-sulfur diesel fuel. A de-sulfuration process in petroleum diesel is needed to ensure the correct operation of after-treatment techniques, but at the cost of decay in the lubricity capability of the fuel. This can be compensated with the addition of biodiesel, even as an additive (at very low concentrations) [10,11].

However, the lubricity of diesel fuel is an essential factor that should be considered before applying the fuel in the automotive industry, as it protects engine moving parts from wear [12]. Diesel fuel injection equipment relies on the lubricating properties of diesel fuel. A lack of lubricity in diesel fuel produces a shortened life of engine components, such as diesel fuel injection pumps and injectors. Furthermore, to prevent surface-to-surface contact and reduce wear under loads, the fuel must have the ability to form a protective film that is indicated by the film percentage in a lubricity analysis [13]. There are two standard methods for determining fuel lubricity: the high-frequency reciprocating rig (HFRR) methods of ASTM D 6079 and the scuffing load ball on cylinder lubricity evaluator (SLBOCLE) of ASTM D 6078. Nevertheless, no absolute correlation has been developed between the two test methods.

1.2. Literature Analysis

The HFRR lubricity tester has become a widespread method for determining diesel fuel lubricity. It is evaluated according to the wear scar diameter (WSD), in microns, produced on an oscillating ball from contact with a stationary disk immersed in the fluid operating under defined and controlled conditions [14]. Generally, the smaller the wear scar, the greater the lubricity of the sample. Therefore, the lubricity analysis also produces a friction coefficient and film percentage. The friction coefficient describes a ratio that defines the force that resists the in-motion contact between two surfaces. This ratio depends on a material's properties, and most materials have a value between zero and one [15]. The higher the lubricity of a fuel, the lower the friction coefficient it has. In the literature, the HFRR method has been used to evaluate the relative effectiveness of diesel fuels for preventing wear under prescribed test conditions. Nevertheless, the correlation of HFRR test results with the field performance of diesel fuel injection systems has not yet been determined. Moreover, the HFRR method is designed to evaluate boundary lubrication properties. Therefore, the friction and wear between two surfaces in relative motion are determined via the surfaces' properties and the contacting fluid's properties. At the same time, the effects of viscosity on lubricity in this test method are not eliminated but only minimized [14,16,17].

During the past several years, many studies have investigated the effects of blending alternatives with diesel fuel on the lubricity characteristics of the fuel blends. Xu et al. [18] successfully characterized emulsified rice husk biodiesel lubricity using an HFRR. The result showed that the bio-oil has better friction reduction and worse wear resistance than diesel fuel. Further examination of the diesel and bio-oil chemical compositions was performed using FTIR. They suggested that the lubricity properties of the emulsified bio-oil were supported by the polar groups and oxygenic compounds that cause the micro-bio-oil

drops to penetrate the surfaces of moving components and produce a chemical reaction that provides lubrication. Meanwhile, the presence of oxygen might increase the corrosion on a surface. Previously, Suarez et al. [19] compared the lubricity of fatty acid mono-alcohol biodiesel, soybean oil pyro-diesel, and their blends with high- and low-sulfur petroleum diesel. Using the HFRR method and a ball-on-disk experiment, it was found that the biodiesel and pyro-diesel lubricities were superior compared with petroleum diesel. Thus, the bio/pyro/diesel blend has better lubricity than petroleum diesel [20,21]. Currently, the sulfur content in ASTM D975 diesel fuel is kept low, to a maximum of 15 ppm, to reduce the emission of sulfur oxides. However, the sulfur content increases wear resistance [8] and fuel oxidation stability [22].

Lubricant tribological properties can be significantly improved by incorporating nano-additives. In general, additives are used to enhance the tribological and thermal properties of a base oil or fluid. Additives such as titanium dioxide, aluminum oxide, zinc oxide, copper and copper oxide, carbon nanotubes, molybdenum disulfide, tungsten disulfide, and diamond improve the heat dissipation rate, load carrying capacity, and wear and friction properties of a base oil or fluid. It is believed that the lubrication mechanisms of lubricant additives include tribofilm formation, the rolling bearing effect, microstructure transformation, and synergistic and repairing effects. Furthermore, their impacts on the environment, safety, and health-related aspects invite more research, and this shows that lubricity research is still very interesting to investigate further [23,24].

The ASTM 7467 standard specification for diesel fuel oil and biodiesel blends (B6–B20) states that they should conform to the requirements of the WSD (using an HFRR) and cannot exceed 520 µm. Meanwhile, according to the requirements for fuels determined in the Worldwide Fuel Charter for category 1, 2, and 3 fuels for compression-ignition engines, the WSD (determined using an HFRR) cannot exceed 460 µm, whereas for category 4 and 5 fuels, this value cannot be greater than 400 µm [17]. The EN 15940 of the European specification for hydrogenated vegetable oil (HVO) limits the WSD to a 460 µm maximum, which is the same value as the HVO specification for Neste Renewable Fuel, while the Crown UK limits it to a 400 µm maximum. Therefore, the lubrication properties of diesel fuel, biodiesel, HVO, and their binary blends are still interesting to be explored regarding the trend of using HFRR test results to determine diesel injection pump distress, which is believed to be a factor in the operation of the component.

1.3. Research Objective

A tribological study of any new fuel blend is important to ensure sustainable engine durability. The main point is the lubricity analysis of all types of renewable fuels, which are important to evaluate and are presented in this study. Moreover, the HFRR test method applies to middle-distillate fuels, which are similar to petroleum-based fuels used in diesel engines, and biodiesel blends. However, the suitability of the HFRR method to analyze the lubricity of HVO and paraffin still needs to be explored. This suitability is related to some of the literature showing that an HVO blend with pure esters allows the isolation of and interference with the effects of each ester molecule to produce positive results on the lubrication capacity.

Our study aimed to determine the effect of the volume of palm oil biodiesel (POB) on the lubricity properties of two types of diesel fuel (DF), i.e., DF with cetane number 48 and a sulfur content maximum of 2000 ppm (DF-CN48), and DF with cetane number 51 and a sulfur content maximum of 500 ppm (DF-CN51), and also hydrogenated vegetable oil (HVO). This study aimed to look into the effect of the methyl ester structure in biodiesel on lubrication improvement, particularly in all-level blends. While previous research has shown that the methyl ester structure positively affects low-lubricity base fuels, little is known about its impact on all-level blends, which could potentially contribute to increased energy security for biodiesel utilization. This research sheds light on the lubricity properties of POB blends with DF and HVO. The novelty of this work mainly lies in the following two aspects. First, we evaluate the suitability of the HFRR method for analyzing the lubricity of

HVO (paraffin) blends, which has not been investigated previously. This is an important aspect that can help to determine if the HFRR method can be used to analyze the lubricity of a wider range of renewable fuels. Second, we investigate the impact of the methyl ester structure in biodiesel on lubrication improvement, particularly in all-level blends. This is a novel aspect, as it has not been extensively explored before, and it has the ability to lead to a rise in energy security for biodiesel use.

2. Materials and Methods

2.1. Materials

In this study, four types of fuels were used to evaluate their lubrication properties. Herein, four fuel types were produced by the major Indonesian fuel and biofuel companies. Two types of commercial diesel fuel, namely, DF-CN48 and DF-CN51, and two types of biofuels, i.e., palm oil biodiesel (POB) and hydrogenated vegetable oil (HVO), were used. The lubricating properties of each binary fuel blend sample were prepared by mixing POB (purity > 98,75%-mass) with DF-CN48, DF-CN51, and HVO, respectively. Herein, each group's mixture and blend were carried out on a volume basis at 28 °C to make several test fuels, i.e., with 10%, 20%, 30%, 40%, 50%, 60%, 70%, 80%, and 90% FAME contents in each fuel test sample. The POB composition for this blend is shown in Table 1 and comprised 43.74%-mass of saturated methyl palmitate, 7.38%-mass of saturated methyl stearate, and 46.34%-mass of unsaturated methyl oleate. Each test sample blend was verified based on its methyl ester content according to the ASTM D7806 method with the interlaboratory development method. All samples comprised the blends' values in the prepared fuel test samples, and the various blends used in this study are listed in Table 2, and the nomenclature is used throughout the manuscript. Fuels were tested immediately after blending to avoid moisture being trapped during long-term storage.

Table 1. Composition of palm oil biodiesel.

Composition	Mass Percentage (%)
Methyl palmitate	43.74
Methyl stearate	7.38
Methyl oleate	46.34
Monopalmitate	0.21
Monostearate	0.08
Monooleate	0.24

Table 2. Methyl ester content in each test sample.

Test Fuel	%-vol Blend	Methyl Ester Content (%-*v*/*v*)		
		DF-CN48	DF-CN51	HVO
B0	0%	0	0	0
B10	10%	10.1	10.2	10.0
B20	20%	19.9	19.8	20.1
B30	30%	30.1	30.0	30.0
B40	40%	40.0	40.0	40.1
B50	50%	50.3	49.8	50.2
B60	60%	61.7	60.2	59.8
B70	70%	72.1	72.4	71.9
B80	80%	83.6	83.5	83.2
B90	90%	87.4	88.7	88.4
B100	100%	98.74 *	98.74 *	98.74 *

* Using gas chromatography.

2.2. Fuel Characterization Test Method

Several characterization techniques were used in this study to investigate the fuel properties of the fuel test samples. The densities of the fuel samples were determined using an automatic density meter in accordance with ASTM D 4052. The kinematic viscosities were determined using an ASTM D 445 capillary tube viscometer with a calibration constant of 40 °C. The cloud points and CFPPs were determined using ASTM D 5773 and ASTM D 6371 using an automatic cloud point and cold filter plugging point analyzer. The acidity of the fuel samples was determined using an ASTM D 664 potentiometric titration method. The oxidation stability of the fuel test samples was determined using the standard method described in EN 15751 during the induction period. In further investigations, the water content was carried out according to ASTM D 6304. The cetane numbers and calorific values were determined using ASTM D 613 and ASTM D 240. Moreover, each test was repeated 3–5 times until the test's repeatability was lower than that stated in the ASTM method, and the average values were taken.

2.3. HFRR Test Method

A high-frequency reciprocating rig (HFRR) instrument (PCS Instrument D-1731) was used to evaluate the fuel lubricity of each test sample according to the ASTM D6079 standard method (Figure 1). Typically, a test specimen ± 2 mL of fuel was placed in the test reservoir of the HFRR. Subsequently, a vibrator arm holding a nonrotating steel ball loaded with a 200 g mass was lowered until it came into contact with a test disk wholly submerged in the fuel. Afterward, the ball was used to rub against the disk with a 1 mm stroke at 50 Hz for 75 min. More specifically, the conditions related to the lubricity test are summarized in Table 3.

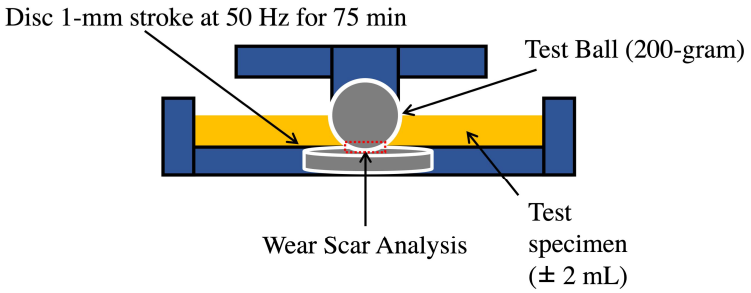

Figure 1. Measuring station of the HFRR lubricity apparatus.

Table 3. Lubricity test conditions.

Parameter	Value
Volume of fuel sample (mL)	2 ± 0.2
Stroke length (mm)	1 ± 0.02
Frequency (Hz)	50 ± 1
Fuel sample temperature (°C)	60 ± 2
Test mass (g)	200 ± 1
Test duration	75 ± 0.1

The test conditions were maintained at 60 °C with a 30% to 85% ambient relative humidity. Later on, the upper specimen holder was removed from the vibrator arm and cleaned. The wear scar was captured using the digital microscope camera. Finally, the friction coefficient was recorded, and the wear scar diameter (WSD) (in µm) was measured by calculating the dimensions of the wear scar on the *x*-axis (WS $_{x\text{-axis}}$) and *y*-axis (WS $_{y\text{-axis}}$) using Equation (1).

$$\text{WSD} = \frac{\text{WS}_{x-\text{axis}} + \text{WS}_{y-\text{axis}}}{2} \quad (1)$$

Uncertainty measurement was conducted to ensure the reliability of the test results. Uncertainty during experiments may be caused by several factors, e.g., the type of instrument, experimental setup, and surrounding conditions. The experiment was performed at least three times for each sample to minimize bias. The uncertainties for each lubricity parameter were determined from the average total uncertainty in the measurement based on determining all the sources of uncertainty that affected the measurement process. The uncertainty values for the friction coefficient, film percentage, and wear scar diameter were ± 0.01, ± 2, and ± 5, respectively.

3. Results and Discussions

3.1. Physiochemical Properties of the Fuel

The physicochemical properties of DF-CN48, DF-CN51, HVO, and POB used in this work are shown in Table 4. As the results show, HVO has a higher cetane number than the other diesel fuels and POB. However, HVO is denser and more viscous than diesel fuel. Meanwhile, POB has a higher water content and acid value than HSD and HVO. Moreover, due to its paraffinic compounds, HVO has greater oxidation stability than POB, which has unsaturated compounds in its methyl ester structure. Moreover, according to the ASTM standard method, distillation characteristics were determined for each base fuel, resulting in a distillation curve based on each base fuel's composition.

Table 4. Physiochemical properties of the base fuels.

Property		POB	DF-CN48	DF-CN51	HVO
Density at 15 °C (kg/m^3)	ASTM D 4052	873	834	837	783
Viscosity at 40 °C (mm^2/s)	ASTM D 445	4.79	3.32	3.14	3.45
Cloud point (°C)	ASTM D 5773	14.8	8.9	1.1	11.1
CFPP (°C)	ASTM D 6371	12	7	−2	9
Distillation range (°C)	ASTM D 86	322–345	145–356	151–355	268–312
Sulfur content (mass %)	ASTM D 4294	<0.001	0.15	0.03	<0.001
Lubricity (microns)	ASTM D 6079	206.5	288.5	453.5	209.5
Water content (mg/kg)	ASTM D 6304	298	87	72	54
Acidity value (mg KOH/g)	ASTM D 664	0.36	0.08	0.05	0.10
Oxidation stability (hours)	EN 15751	17	>180	>180	>180
Higher heating value (MJ/kg)	ASTM D 240	41.410	45.215	45.660	47.050
Cetane number	ASTM D 613	57	48	51	>75

The typical distillation curves of the test fuels are shown in Figure 2. In principle, hydrocarbons outside of the presented boiling range are also suitable for the combustion of diesel. DF-CN48 and DF-CN51 have a wide boiling point range, which can be divided into 3 sections: a light fraction (10% distilled T10), a medium fraction (50% distilled T50), and a heavy fraction (90% distilled T90). The results show that DF-CN48 and DF-CN51 have broad distillation curves caused by containing various hydrocarbon compounds as components. Furthermore, POB and HVO have flat curves compared with DF-CN48 and DF-CN51. It is clear that biodiesel has a major methyl ester component with a boiling range of 322–345 °C, and HVO has a major paraffinic compound component with a boiling range of 268–312 °C.

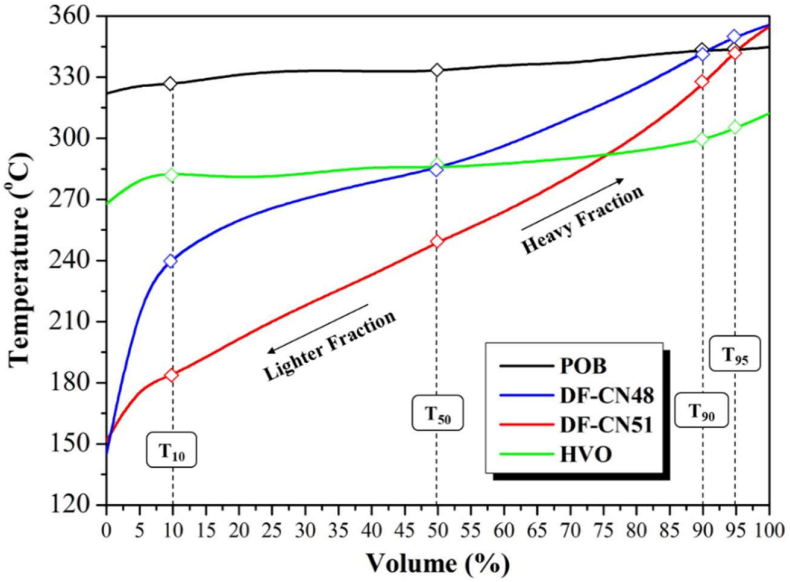

Figure 2. Distillation curves of POB, DF-CN48, DF-CN51, and HVO.

3.2. Friction Behavior Analysis

Figure 3 shows the friction behavior of DF-CN48, which was influenced by the POB percentages in the blends. It can be seen that the friction coefficient fluctuated during the test time. Based on the results, the friction coefficient value decreased with an increasing POB percentage in DF-CN48 due to the lubricating properties of the methyl ester compounds. Specific confirmation of the positive impact of POB on the lubricity of diesel fuel is found in the research conducted by Lapuerta et al. [25]. Adding 10% biodiesel to e-diesel (7.7% ethanol v/v in diesel fuel) reduces the corrected WSD from 327 µm to 275 µm compared with pristine e-diesel (without % biodiesel v/v).

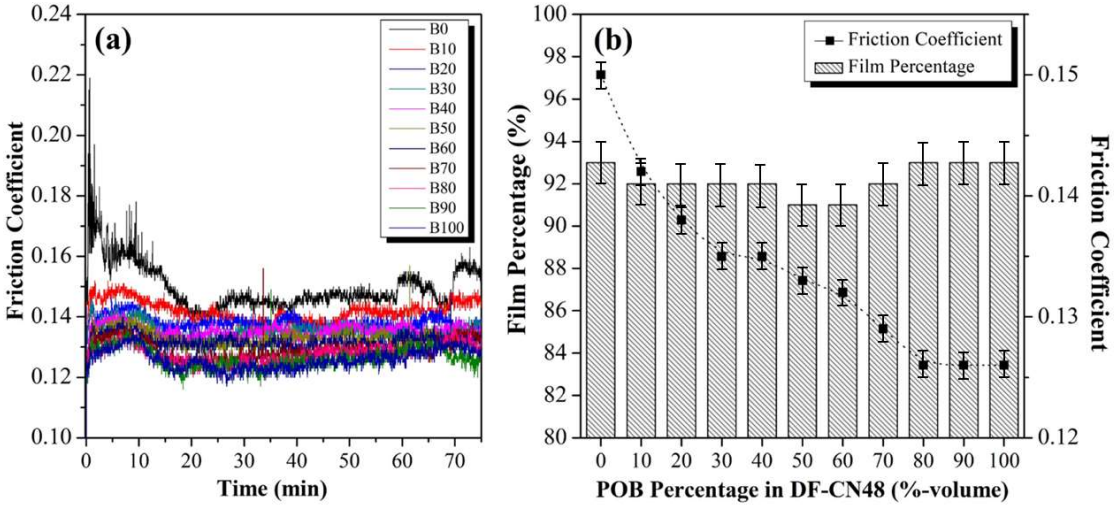

Figure 3. Effect of the POB volume (Bxx) in DF-CN48 blends on their (**a**) friction behavior and (**b**) average friction coefficients and film percentages.

The highest average friction coefficient value is 0.150, which is the average friction coefficient for DF-CN48, and the lowest is for POB, with an average friction coefficient value of 0.126. The friction coefficient value with an increasing POB percentage looks tenuous, even though there are some points at specific minutes whose values are close together. From Figure 3, it can be analyzed that the film percentage value is not directly proportional or inversely proportional to the POB volume in DF-CN48, in contrast with the

friction coefficient value, which decreases with the addition of POB to DF-CN48. According to Mei et al. and Sundus et al. [26,27], the decrease in the friction coefficient with the increasing POB percentage could be attributed to the methyl ester compound in the DF-CN48 blend. The ester group in POB has lubrication properties whereby they are adsorbed on the metal surface to soften the friction [26]. Interestingly, increasing levels of POB in DF-CN48 resulted in smoother WSD values and smaller diameters. This phenomenon is due to the adsorption of ester molecules on the metallic surfaces, which acted as a protective layer during the rubbing process [13,28].

Figure 4 shows the values of the friction coefficients, which decrease with an increasing volume of POB. It is clear that methyl esters have high lubricating properties, resulting in a reduced friction coefficient and increased film percentage with the effect of the POB volume in DF-CN51. Based on the results, DF-CN51 has the highest friction coefficient value with an average of 0.293 compared with the POB friction coefficient of 0.126. The experimental results show that adding biodiesel decreases the friction coefficient from 0.30 to 0.14–0.12 for B10–B90. It is worth noting that having no lubricating film between the contacting surfaces during the test led to a very high friction coefficient for DF-CN51. After adding POB, steady-state conditions were achieved due to it forming a thin lubricating protective layer between the metallic surfaces, leading to a lower friction coefficient. The pure POB sample showed a minimum friction coefficient due to the adsorption of ester molecules on the metallic surfaces, which acted as a protective layer during the rubbing process [29,30]. It is clear that the ester molecules in POB in the DF-CN51 fuel samples assisted in forming a protective lubricating film between the contacting surfaces. From Figures 3 and 4, it is evident that POB acts as a lubricant additive and a friction modifier for diesel fuel (DF-CN48 and DF-CN51) based on the principle of film formation on metal surfaces. On these protected engine components, the lubricant additive has a mechanism of being adsorbed on the surfaces to reduce the friction coefficient of the engine components in contact with each other [17,31].

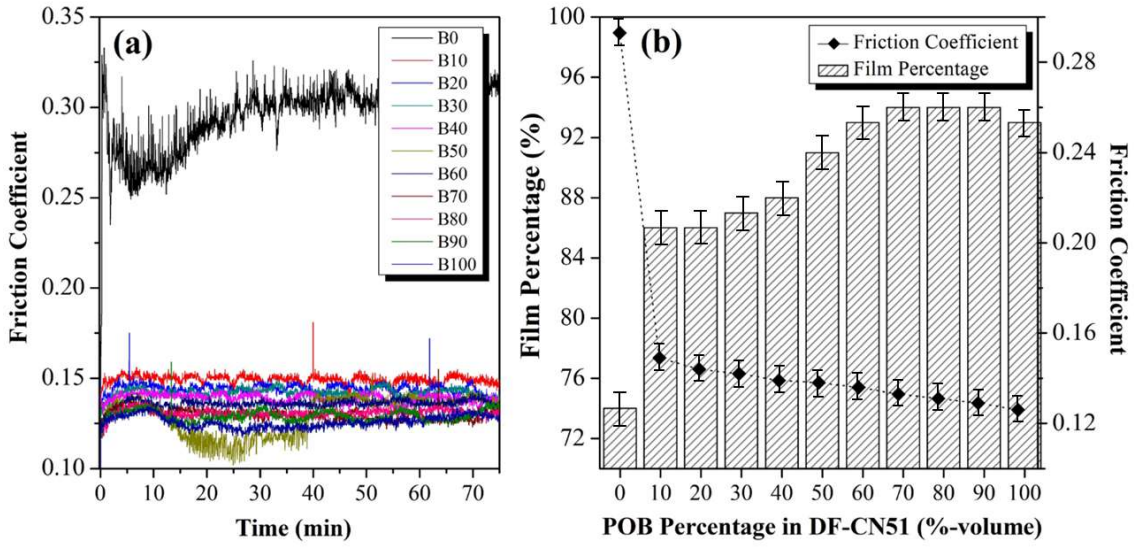

Figure 4. Effect of the POB volume (Bxx) in DF-CN51 blends on their (**a**) friction behavior and (**b**) average friction coefficients and film percentages.

The effect of biodiesel in HVO on the fuel's lubrication properties is shown in Figure 5. An interesting trend was found in the friction coefficient value with the increasing POB content in the HVO. However, it is worth noting that a non-equal contribution towards the friction coefficient was also observed when the POB concentration was beyond 60–90%-*v*/*v*. As a result, pristine HVO has a friction coefficient of 0.125, and the value decreases gradually to the lowest at B30 with a friction coefficient of 0.121. At B40, the friction coefficient value increases gradually until the highest value at B80 of 0.128. The film percentage produced

with B0 is 93%, the same as that with B100, and increases for B10, B20, B30, B40, and B50 with a film percentage of 95%. Then, the film percentage decreases to 91% for B60, B70, B80, and B90. Based on the results, 10–50% POB blends in HVO showed noticeable lubricity improvements with friction coefficients lower than that for pristine HVO. According to the literature, mixing biodiesel and HVO must produce effective lubricity properties to prevent the removal of the adsorbed film formed under low-stress conditions at the test temperature and load. Nevertheless, the higher ester content in POB-HVO blends did not contribute to the lubricity capacities of the fuel blends (for 60–90% POB). It is clear that a change in the saturation degree in higher-POB blends did not cause a strong improvement in the HVO blends' lubricity capacities [12,28].

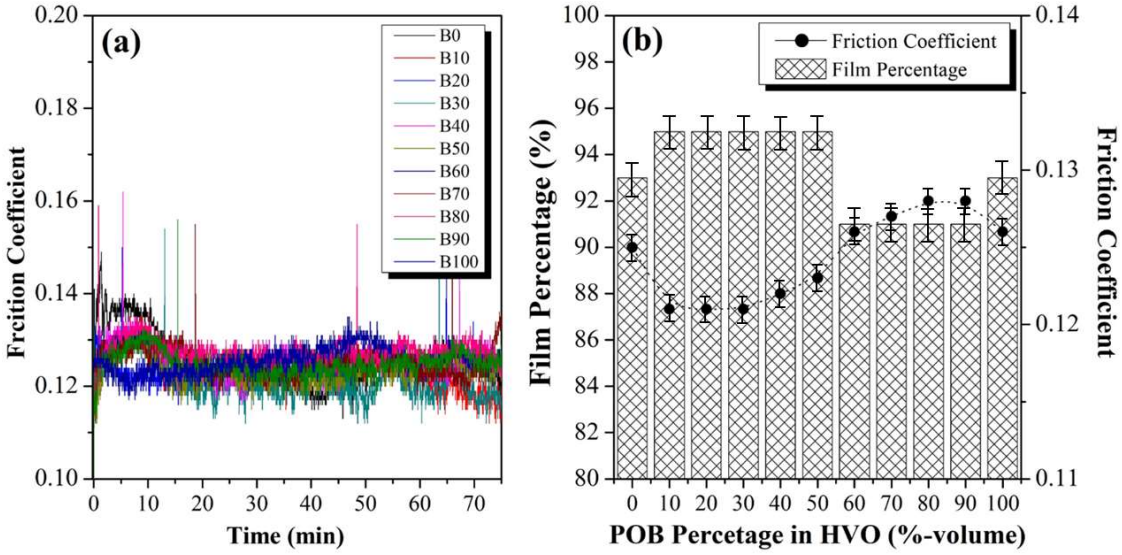

Figure 5. Effect of the POB volume (Bxx) in HVO blends on their (**a**) friction behavior and (**b**) average friction coefficients and film percentages.

3.3. Wear Characteristics

The wear characteristics of each fuel blend sample in the HFRR test occurred on the surface of the test material on a friction node determined by the physical processes. The appearance of the wear scar on a ball can vary with the fuel type, particularly when lubricity additives are present. The wear scar appears to be a series of scratches in the ball's direction of motion, somewhat larger in the x direction than in the y direction. In some cases, for example, when low-lubricity reference fluids are tested, the boundary between the scar and the discolored (but unworn) area of the ball is distinct, and it is easy to measure the scar size. In other cases, the central scratched part of the scar is surrounded by less distinct wear, and there is no sharp boundary between the worn and unworn areas of the ball, and it shows cracks in different directions.

An increase in the methyl ester (POB) in the diesel fuels (DF-CN48 and DF-CN51) increased the oxygen molecules in the samples. The presence of oxygen is conducive to tribochemical processes, which, in turn, leads to a change in the chemical and phase composition of the material [13,32]. It is clear that the evolution of the chemicals and phases led to metal oxides forming and a reduction in the friction coefficient of the friction node. The lubricating properties of generated metal oxides and their mixtures are determined by their ionic potentials, as pointed out in [15,33,34]. A higher ionic potential carries out a stronger polarization effect leading to a lower friction coefficient. Low ionic potential in fuel can increase the friction coefficient and intensify wear, with a higher wear scar diameter (WSD) value [8,35]. According to Kuszewski et al. [17], at low oxygen concentrations in a sample, the wear is decreased by the oxygen due to the formation of anti-adhesive oxide layers. Higher concentrations lead to excessive oxidation of the friction surface,

leading to more intensification of wear. However, the wear characteristics phenomenon in the POB blends in DF-CN48 and DF-CN51 were associated with the anti-adhesive oxide layer formation and wear resistance increase at the beginning of the test. Clearly, such a phenomenon is dominant in generating wear scars [36,37]. As shown in Figures 6–8, confirmation of the tribochemical reactions within the test friction pair is given in the photographs showing wear scars on the test balls. The effect of POB addition into DF-CN48, DF-CN51, and HVO was analyzed for its degree of conformity correlation with the WSD formation and its significance model to evaluate the results further.

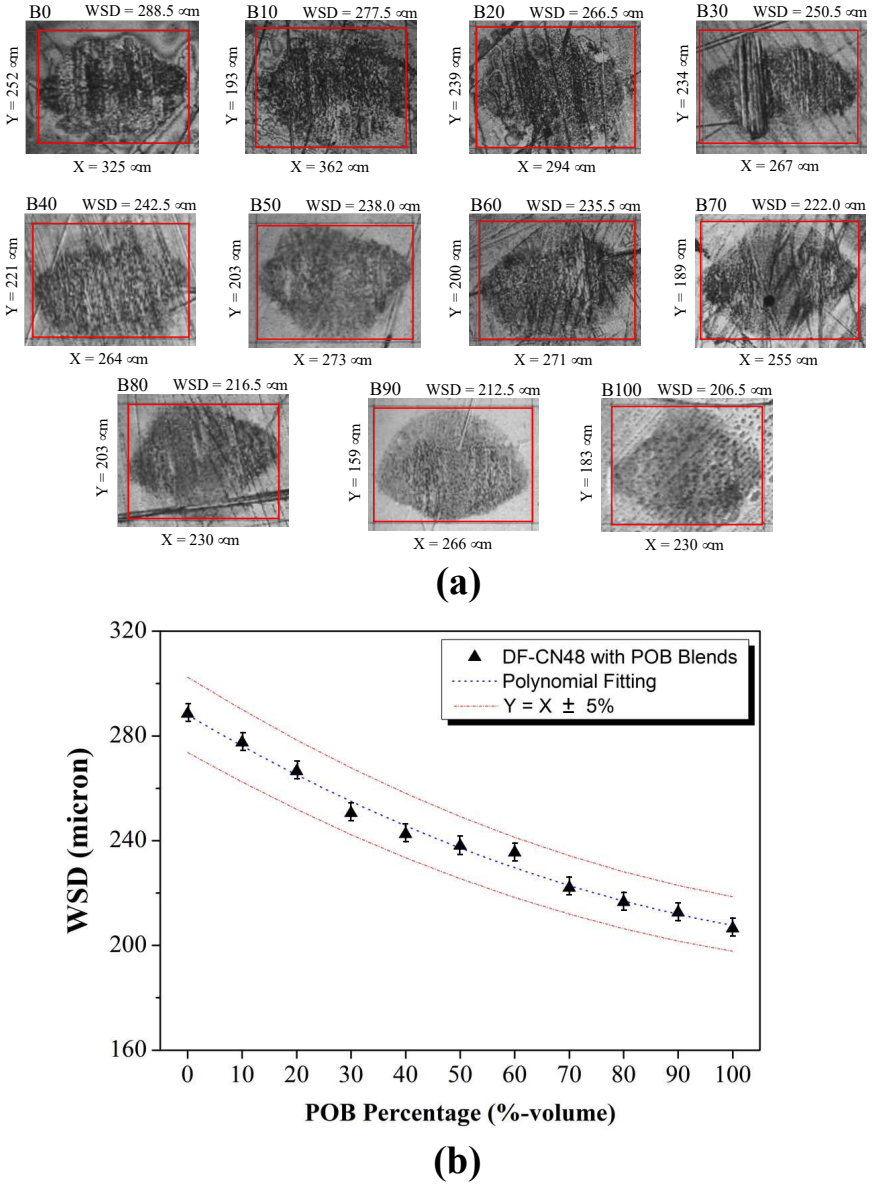

Figure 6. Effect of POB percentage on (**a**) WSD photographs (red lines are the wear scar measurement guides) and (**b**) WSD values of DF-CN48 blends with POB percentages (Bxx).

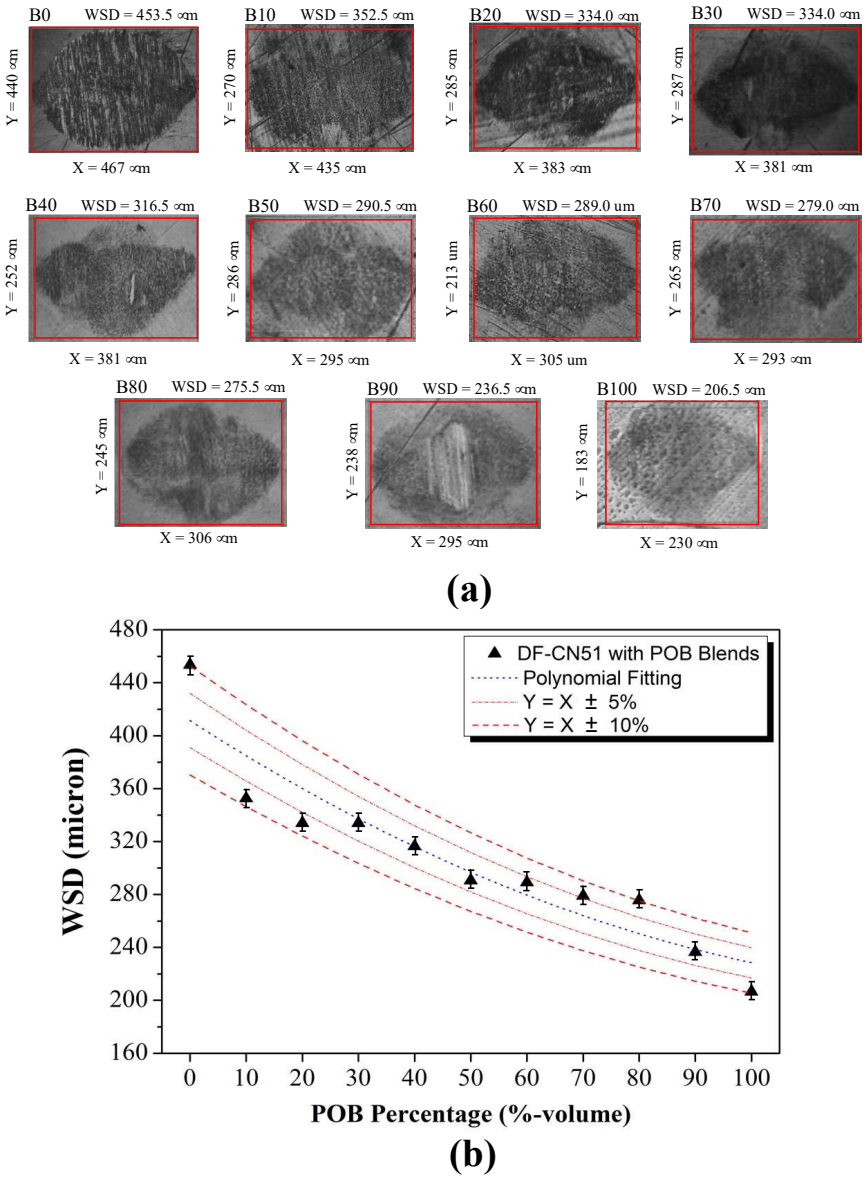

Figure 7. Effect of POB percentage on (**a**) WSD photographs (red lines are the wear scar measurement guides) and (**b**) WSD values of DF-CN51 blends with POB percentages (Bxx).

Figure 6 shows the wear scars produced with each additional volume of POB in DF-CN48. The results show decreased WSD values when increasing the POB volume in DF-CN48. Successively, rising levels of POB in DF-CN48 resulted in smoother WSD values and smaller diameters. DF-CN48 has an immense WSD value of 288.5 µm, which decreases with the POB volume in DF-CN48. Meanwhile, the smallest value of the wear scar diameter with POB is 206.5 µm, with a smooth and precise WSD character. Clearly, every 10%-v/v addition of POB to DF-CN48 results in a 3% decrease in WSD formation. As shown in Figure 6, the addition of biodiesel improved the lubricity of DF-CN48, with a polynomial fitting chosen for the generated model. Furthermore, the calculated R^2 value (0.9951) of the polynomial fitting was also considerably high and considered to be in good agreement. It is clear that all the DF-CN48 and biodiesel blends following the model satisfy the limit of ±5%.

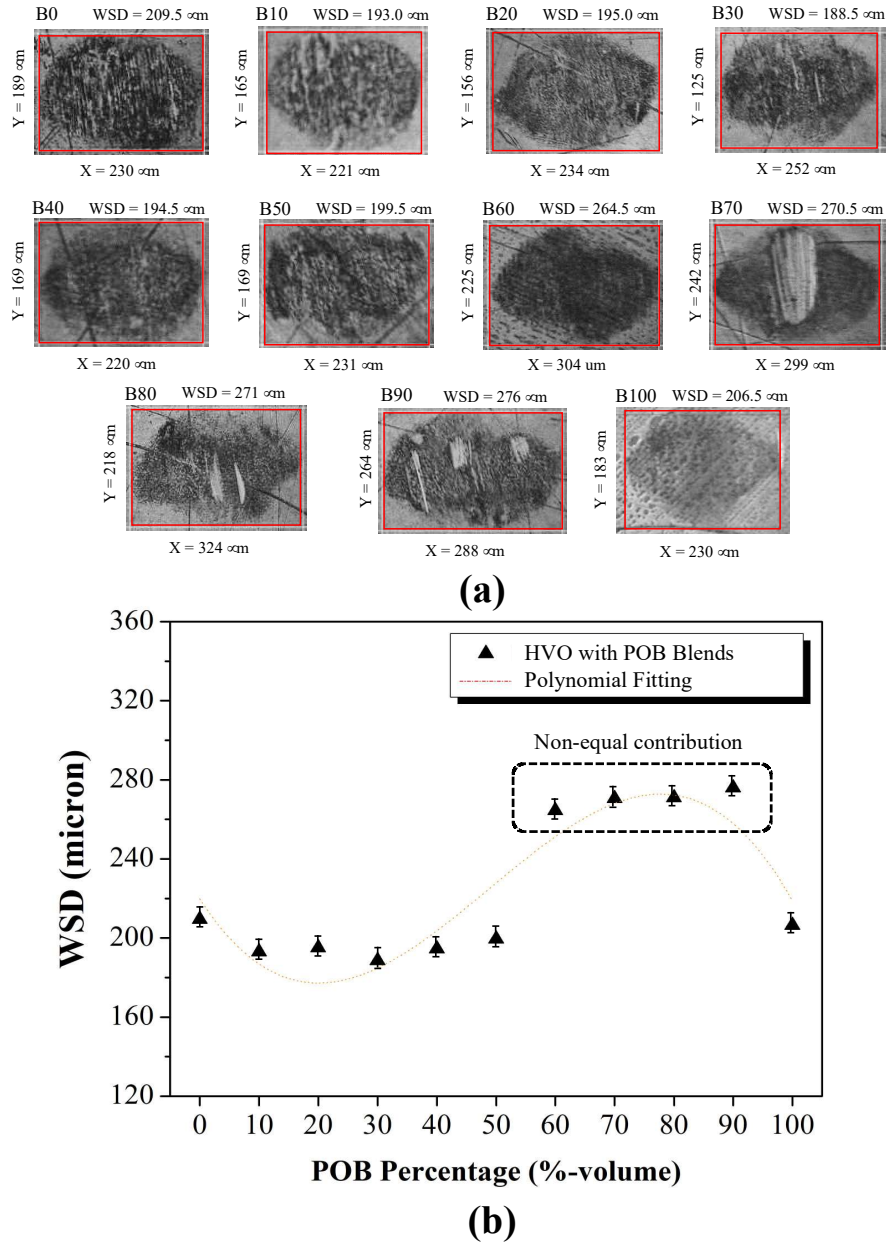

Figure 8. Effect of POB percentage on (**a**) WSD photographs (red line is the wear scar measurement guide) and (**b**) WSD values of HVO blends with POB percentages (Bxx).

The wear scar characteristics resulting from the variation in POB in DF-CN51 are shown in Figure 6. The wear scar looks more precise and smoother with the increase in POB in DF-CN51. Methyl ester is an active compound that can become concentrated on a metal surface, forming a thin adsorbed layer. The coating can naturally change the molecular structure (via intermolecular forces) and surface characteristics of the metal. It causes a change in the process kinetics involved in transferring substances across the surfaces that rub against each other [13,15]. As a result, an increase in POB in DF-CN51, results in a change in the conditions of the molecular interactions between the two contacting surfaces and their effect on minimizing WSD formation [13,17]. It is worth noting that adding the first 10%-v/v biodiesel to DF-CN51 resulted in the optimal WSD improvement, with a decrease of 22%. Adding 10% POB further reduced WSD formation by 2–7% (B20–B90). These results indicate that the effect of biodiesel as a lubricant improver additive is very influential on the type of fuel used. In this study, DF-CN48 and DF-CN51 have differences

in their compositional hydrocarbon compositions, which are determined via the differences in their distillation ranges, as shown in Figure 1. For further analysis, the polynomial fitting expresses the effect of biodiesel addition on DF-CN51, as demonstrated in Figure 7. According to the results, the model's calculated R^2 value (0.8828) is considerably high, implying that the model accurately navigates the correlations of all the samples following it satisfying the limit of ±10%.

Figure 8 shows that increasing the WSD increased the percentage of POB in the HVO mixture. The wear scar character in the HVO mixture tends to be longer and smoother as the percentage of the POB volume increases. Many dominant vertical strokes are found on B70, B80, and B90. The test results show that biodiesel in HVO only affects the WSD by 1–3% (B10–B50). However, it is worth noting that a non-equal contribution to the WSD was also observed when the POB concentration was beyond 60–90%-v/v. These results suggest optimizing biodiesel as an additive improver to increase the effectiveness of the material's lubricity is imperative. According to [17,29], compounds with good lubrication properties are adsorbed as thin layers on metal surfaces. These layers can be easily cut off and easily distracted by rough moving surfaces. The most exciting thing is that all these compounds (methyl esters) function via adsorption on the metal surface, and the adsorbed layer can be easily removed due to friction on the rough surface. After removing the stress, the adsorbed layer can return to its original position [7]. This phenomenon can be described in the experimental results of the POB-HVO blends. In such a non-ideal mixture, the methyl ester in POB and the paraffinic compounds in HVO show effects of lubricity that compete determinatively and attractively with each other, resulting in a non-ideal contribution to the friction coefficient and WSD value.

According to the requirements for fuels determined in the Worldwide Fuel Charter for category 1, 2, and 3 fuels for compression-ignition engines, the WSD (determined using an HFRR) cannot exceed 460 µm, whereas for category 4 and 5 fuels, this value cannot be greater than 400 µm. Thus, all the blends of DF-CN48 and HVO with POB in Figure 8 meet the requirements for all fuel categories for compression-ignition engines. Interestingly, with POB blends, DF-CN51 can fulfill the requirement in the WWFC, whereby pristine DF-CN51 has the highest WSD (467 µm).

Table 5 summarizes the results of a generated model using ANOVA analysis. The ANOVA suggested that the polynomial model was the best based on the results. It represents the relationship between the lubrication properties of the fuel test samples (Y) and the concentration of POB (x). As shown in Table 3, the calculated F-value for the generated model of each blend of DF-CN48, DF-CN-51, and HVO with POB was 402.85, 57.51, and 19.10, respectively. The results indicate that the model is significant, with a 0.01% chance of occurring due to noise. Furthermore, the considerable values of the error probability (P) were also found to be less than 0.05 (<0.0001 for DF-CN48 and DF-CN51 with POB blends and <0.005 for HVO with POB blends). This suggests that the addition of POB blends significantly affects the values of the DF and HVO blends' wear scars with a probability level of 95%. Therefore, the generated polynomial model is sufficient for describing the fuels' lubrication properties.

Table 5. Analysis of variance (ANOVA) results for fuel test lubricity.

Fuel Blends Sample	Model	F-Value	*P*	R^2	Adj. R^2
DF-CN48 with POB blends	Polynomial	402.85	<0.0001	0.9951	0.9877
		$Y = 0.0043x^2 - 1.229x + 288.06$			
DF-CN51 with POB blends	Polynomial	57.51	<0.0001	0.8828	0.8535
		$Y = -0.0092x^2 - 2.7522x - 411.44$			
HVO with POB blends	Polynomial	19.10	<0.005	0.9629	0.8786
		$Y = -0.001x^3 - 0.146x^2 - 4.647x + 219.74$			

The specific wear rate for each fuel blend was determined in this study according to the literature [11]. The specific wear rates (W_{ball}) were calculated as per Equations (2)–(4):

$$V_{ball} = \frac{\pi h}{6}\left(\frac{3d^2}{4} + h^2\right) \quad (2)$$

$$h = r - \sqrt{r^2 - \frac{d^2}{4}} \quad (3)$$

$$W_{ball} = \frac{V_{ball}}{NS} \quad (4)$$

where d is the average wear scar diameter on rubbed balls, r is the tested ball radius, S is the sliding distance, and N is the normal load. Figure 9 shows the impact of frictional species growth kinetics on the surface material wear. According to the results, DF-CN48, DF-CN51, and HVO have specific wear rates of 126, 311, and 66 $\mu m^3/Nm$, respectively (where pristine POB has the lowest specific wear rate of 64 $\mu m^3/Nm$). The addition of POB decreased the specific wear rate. As a result, the POB used in this work contains methyl ester compounds that act as lubricity improvers, leading to the lower typical wear rates measured in DF-CN48, DF-CN51, and HVO. It is clear that the specific wear rates correlate linearly with the wear scar diameters and friction coefficients. The lower the friction coefficient of the fuel blends, the lower the wear diameter and specific wear rate they have, signifying the higher lubricity of the fuels.

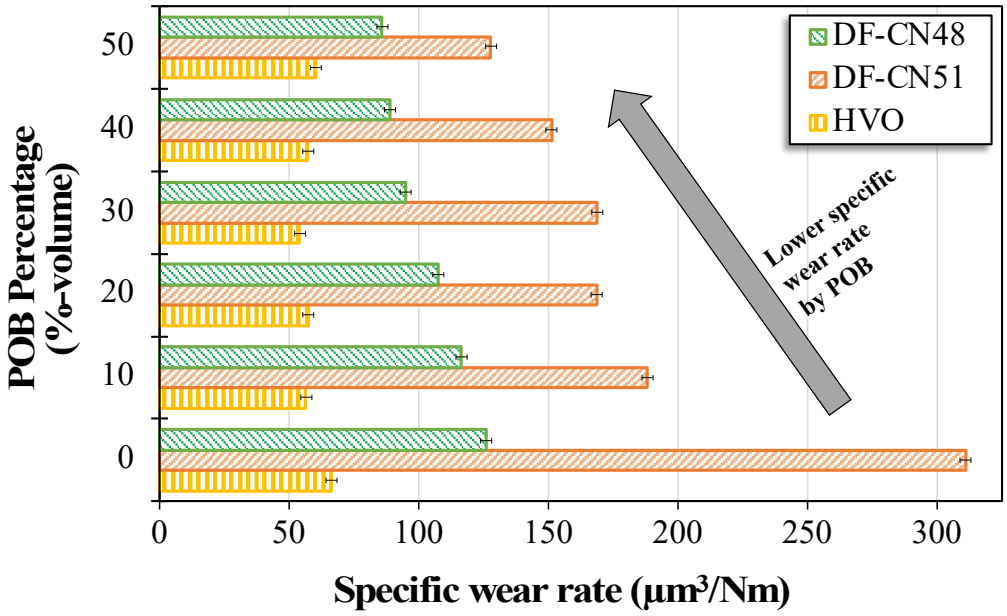

Figure 9. Specific wear rate of surface lubricated with POB blends in different concentrations.

4. Conclusions

This work comprehensively presented a lubricating properties investigation on the effects of POB blends in diesel fuel (DF-CN48 and DF-CN51) and HVO. Based on the results, the addition of POB successfully improved the lubricating properties of the DF-CN48 and DF-CN51 fuel samples. The key points of the results indicate the ability of POB to act as a lubricity improver, efficiently showing a minimum friction coefficient due to the adsorption of ester molecules on the metallic surfaces, which act as a protective layer during the rubbing process. This phenomenon was indicated in the more positive film percentage and the specific wear rate decrease. Such a phenomenon was obtained due to the ability of the ester molecules in POB to assist the protective lubricating film formation between the

contacting surfaces. The results demonstrated that an increase in the POB blend in DF-CN48 and DF-CN51 resulted in a change in the conditions of the molecular interactions between the two contacting surfaces and the effect of minimizing WSD formation. Meanwhile, adding 10%-v/v POB to DF-CN51 resulted in the optimum WSD improvement, with a decrease of 22%. However, adding 10% POB to DF-CN48 decreased the WSD by 3%, linearly. These results indicate that the effect of biodiesel as a lubricant improver additive is very influential on the type of fuel used. Interestingly, the methyl ester in POB and paraffinic compounds in HVO show lubrication effects that compete determinatively and attractively with each other with 60–90%-v/v of POB. Consequently, the POB-HVO blends at these levels have non-ideal contributions to the friction coefficients and WSD values. The results demonstrate that adding POB blends significantly affects the values of DF and HVO blend wear scars with a probability level of 95%. Therefore, the generated polynomial model is sufficient for describing the fuels' lubrication properties. Future research should consider field testing under real-world conditions to confirm the findings of this study and consider the full life-cycle environmental impacts of biodiesel use to determine its sustainability.

Author Contributions: Conceptualization, C.S.W. and N.A.F.; methodology, L.A.; software, N.A.F. and A.S.A.; validation, C.S.W. and A.S.A.; formal analysis, N.A.F. and R.Z.; investigation, R.Z. and L.A.; resources, M.; data curation, N.A.F. and R.Z.; writing—original draft preparation, N.A.F. and A.S.A.; writing—review and editing, A.S.A. and N.A.F.; visualization, R.A.; supervision, C.S.W.; project administration, R.A. All authors have read and agreed to the published version of the manuscript.

Funding: This research and the APC were funded by the Oil Palm Plantation Fund Management Agency (BPDPKS) Indonesia under the BPDP Sawit Grant 2022 (PRJ-327/DPKS/2022).

Data Availability Statement: The data presented in this study are available on request from the corresponding author. The data are not publicly available due to privacy reasons.

Acknowledgments: The authors would like to express their gratitude and highest appreciation to the NRE-Biofuel Laboratory, the Department of Product Application Technology, at the Research and Development Centre for Oil and Gas Technology "LEMIGAS" for their support in this research. And the authors also would like to express our sincere gratitude and highest appreciation to The Directorate General of the New, Renewable Energy and Energy Conservation Department, Ministry of Energy and Mineral Resources, Oil Palm Plantation Fund Management Agency (BPDPKS) Indonesia, PERTAMINA, APROBI, BRIN, and IKABI for their support in this project.

Conflicts of Interest: The authors declare no conflict of interest.

Abbreviations

The following abbreviations are used in this manuscript:

Bxx	Biodiesel blends (xx %-volume)
DF-CN48	Diesel fuel with cetane number 48
DF-CN51	Diesel fuel with cetane number 51
HFRR	High-frequency reciprocating rig
HVO	Hydrogenated vegetable oil
POB	Palm oil biodiesel
WSD	Wear scar diameter
WWFC	Worldwide Fuel Chapter

References

1. Aghbashlo, M.; Peng, W.; Tabatabaei, M.; Kalogirou, S.A.; Soltanian, S.; Hosseinzadeh-Bandbafha, H.; Mahian, O.; Lam, S.S. Machine learning technology in biodiesel research: A review. *Prog. Energy Combust. Sci.* **2021**, *85*, 100904. [CrossRef]
2. Canakci, M.; Sanli, H. Biodiesel production from various feedstocks and their effects on the fuel properties. *J. Ind. Microbiol. Biotechnol.* **2008**, *35*, 431–441. [CrossRef] [PubMed]
3. Monirul, I.M.; Masjuki, H.H.; Kalam, A.; Zulkifli, N.W.M.; Rashedul, H.K.; Rashed, M.M.; Imdadul, H.K.; Mosarof, M.H. A comprehensive review on biodiesel cold flow properties and oxidation stability along with their improvement processes. *RSC Adv.* **2015**, *5*, 86631–86655. [CrossRef]

4. Mukherjee, I.; Sovacool, B.K. Palm oil-based biofuels and sustainability in southeast Asia: A review of Indonesia, Malaysia, and Thailand. *Renew. Sustain. Energy Rev.* 2014. [CrossRef]
5. Farobie, O.; Hartulistiyoso, E. Palm Oil Biodiesel as a Renewable Energy Resource in Indonesia: Current Status and Challenges. *Bioenergy Res.* **2022**, *15*, 93–111. [CrossRef]
6. Fathurrahman, N.A.; Wibowo, C.S.; Bethari, S.A.; Anggarani, R.; Aisyah, L.; Maymuchar. Fuel Properties of Two Types High-Speed Diesel Blending with Palm Oil Biodiesel in Indonesia. *IOP Conf. Ser. Earth Environ. Sci.* **2021**, *749*, 012030. [CrossRef]
7. Muñoz, M.; Moreno, F.; Monné, C.; Morea, J.; Terradillos, J. Biodiesel improves lubricity of new low sulphur diesel fuels. *Renew. Energy* **2011**, *36*, 2918–2924. [CrossRef]
8. Hsieh, P.Y.; Bruno, T.J. A perspective on the origin of lubricity in petroleum distillate motor fuels. *Fuel Process. Technol.* **2015**, *129*, 52–60. [CrossRef]
9. Kuronen, M.; Mikkonen, S.; Aakko, P.; Murtonen, T. *Hydrotreated Vegetable Oil as Fuel for Heavy Duty Diesel Engines*; SAE International: Warrendale, PA, USA, 2007. [CrossRef]
10. Ababneh, H.; Mohammad, N.; Choudhury, H.A.; Zhang, L.; Gani, R.; McKay, G.; Elbashir, N. Enhancing the lubricity of gas-to-liquid (GTL) paraffinic kerosene: Impact of the additives on the physicochemical properties. *BMC Chem. Eng.* **2020**, *2*, 1–16. [CrossRef]
11. Hong, F.T.; Singh, E.; Sarathy, S.M. On the origins of lubricity and surface cleanliness in ethanol-diesel fuel blends. *Fuel* **2021**, *302*, 121135. [CrossRef]
12. Dodos, G.S.; Vassileiou, F.; Karonis, D. *Lubricity of Diesel Fuel Hydrocarbons and Surrogate Fuels*; SAE International: Warrendale, PA, USA, 2017. [CrossRef]
13. Hu, Z.; Zhang, L.; Li, Y. Investigation of tall oil fatty acid as antiwear agent to improve the lubricity of ultra-low sulfur diesels. *Tribol. Int.* **2017**, *114*, 57–64. [CrossRef]
14. Nikanjam, M.; Rutherford, J. *Improving the Precision of the HFRR Lubricity Test*; SAE International: Warrendale, PA, USA, 2006.
15. Azad, A.K.; Rasul, M.G.; Sharma, S.C.; Khan, M.M.K. The lubricity of ternary fuel mixture blends as a way to assess diesel engine durability. *Energies* **2018**, *11*, 33. [CrossRef]
16. Knothe, G. Evaluation of ball and disc wear scar data in the HFRR lubricity test. *Lubr. Sci.* **2008**, *20*, 35–45. [CrossRef]
17. Kuszewski, H.; Jaworski, A.; Ustrzycki, A. Lubricity of ethanol–diesel blends—Study with the HFRR method. *Fuel* **2017**, *208*, 491–498. [CrossRef]
18. Xu, Y.; Wang, Q.; Hu, X.; Li, C.; Zhu, X. Characterization of the lubricity of bio-oil/diesel fuel blends by high frequency reciprocating test rig. *Energy* **2010**, *35*, 283–287. [CrossRef]
19. Suarez, P.A.Z.; Moser, B.R.; Sharma, B.K.; Erhan, S.Z. Comparing the lubricity of biofuels obtained from pyrolysis and alcoholysis of soybean oil and their blends with petroleum diesel. *Fuel* **2009**, *88*, 1143–1147. [CrossRef]
20. Douvartzides, S.L.; Charisiou, N.D.; Papageridis, K.N.; Goula, M.A. Green diesel: Biomass feedstocks, production technologies, catalytic research, fuel properties and performance in compression ignition internal combustion engines. *Energies* **2019**, *12*, 809. [CrossRef]
21. Kumaravel, S.T.; Murugesan, A.; Vijayakumar, C.; Thenmozhi, M. Enhancing the fuel properties of tyre oil diesel blends by doping nano additives for green environments. *J. Clean. Prod.* **2019**, *240*, 118128. [CrossRef]
22. Auzani, A.S.; Clements, A.G.; Hughes, K.J.; Ingham, D.B.; Pourkashanian, M. Assessment of ethanol autoxidation as a drop-in kerosene and surrogates blend with a new modelling approach. *Heliyon* **2021**, *7*, e07295. [CrossRef]
23. Singh, A.; Verma, N.; Mamatha, T.G.; Kumar, A.; Singh, S.; Kumar, K. Properties, functions and applications of commonly used lubricant additives: A review. In *Materials Today: Proceedings*; Elsevier Ltd.: Amsterdam, The Netherlands, 2020; pp. 5018–5022. [CrossRef]
24. Zhao, J.; Huang, Y.; He, Y.; Shi, Y. Nanolubricant additives: A review. *Friction* **2021**, *9*, 891–917. [CrossRef]
25. Lapuerta, M.; García-Contreras, R.; Agudelo, J.R. Lubricity of ethanol-biodiesel-diesel fuel blends. *Energy Fuels* **2010**, *24*, 1374–1379. [CrossRef]
26. Mei, D.; Dai, S.; Chen, T.; Wang, H.; Yuan, Y. Absorption of fuel containing esters on iron surface based on molecular simulation and its effects on lubricity. *Energy Sources Part A Recovery Util. Environ. Eff.* **2020**, 1–12. [CrossRef]
27. Sundus, F.; Fazal, M.A.; Masjuki, H.H. Tribology with biodiesel: A study on enhancing biodiesel stability and its fuel properties. *Renew. Sustain. Energy Rev.* **2017**, *70*, 399–412. [CrossRef]
28. Rodríguez-Fernández, J.; Ramos, A.; Sánchez-Valdepeñas, J.; Serrano, J.R. Lubricity of paraffinic fuels additivated with conventional and non-conventional methyl esters. *Adv. Mech. Eng.* **2019**, *11*, 1687814019877077. [CrossRef]
29. Hu, J.; Du, Z.; Li, C.; Min, E. Study on the lubrication properties of biodiesel as fuel lubricity enhancers. *Fuel* **2005**, *84*, 1601–1606. [CrossRef]
30. Crockett, R.M.; Derendinger, M.P.; Hug, P.L.; Roos, S. Wear and electrical resistance on diesel lubricated surfaces undergoing reciprocating sliding. *Tribol. Lett.* **2004**, *16*, 187–194. [CrossRef]
31. Voice, A.K.; Tzanetakis, T.; Traver, M. *Lubricity of Light-End Fuels with Commercial Diesel Lubricity Additives*; SAE International: Warrendale, PA, USA, 2017. [CrossRef]
32. Mujtaba, M.; Masjuki, H.; Kalam, M.; Noor, F.; Farooq, M.; Ong, H.C.; Gul, M.; Soudagar, M.E.M.; Bashir, S.; Fattah, I.R.; et al. Effect of additivized biodiesel blends on diesel engine performance, emission, tribological characteristics, and lubricant tribology. *Energies* **2020**, *13*, 3375. [CrossRef]

33. Lehto, K.; Vepsäläinen, A.; Kiiski, U.; Kuronen, M. Diesel Fuel Lubricity Comparisons with HFRR and Scuffing Load Ball-on-Cylinder Lubricity Evaluator Methods. *SAE Int. J. Fuels Lubr.* **2014**, *7*, 842–848. [CrossRef]
34. Uchôa, I.M.A.; Neto, A.A.D.; Da Silva Santos, E.; De Lima, L.F.; De Barros, E.L. Neto Evaluation of lubricating properties of diesel based fuels micro emulsified with glycerin. *Mater. Res.* **2017**, *20*, 701–708. [CrossRef]
35. Lapuerta, M.; Sánchez-Valdepeñas, J.; Sukjit, E. Effect of ambient humidity and hygroscopy on the lubricity of diesel fuels. *Wear* **2014**, *309*, 200–207. [CrossRef]
36. Peng, D.X. The effect on diesel injector wear, and exhaust emissions by using ultralow sulphur diesel blending with biofuels. *Mater. Trans.* **2015**, *56*, 642–647. [CrossRef]
37. De Farias, A.C.M.; De Medeiros, J.T.N.; Alves, S.M. Micro and nanometric wear evaluation of metal discs used on determination of biodiesel fuel lubricity. *Mater. Res.* **2014**, *17*, 89–99. [CrossRef]